Schweizerische Eidgenossenschaft
Confédération suisse
Confederazione Svizzera
Confederaziun svizra

Federal Department of the Environment, Transport, Energy and Communications DETEC

Swiss Federal Office of Energy SFOE
Energy Research and Cleantech Division

Final report dated 05.12.2022

Reliability of PV Systems integrated in the built environment (BIPV)

Source: ©www.bipv.ch 2020

University of Applied Sciences and Arts
of Southern Switzerland

SUPSI

Date: 05.12.2022

Location: Bern

Publisher:
Swiss Federal Office of Energy SFOE
Energy Research and Cleantech
CH-3003 Bern
www.bfe.admin.ch

Co-financing:
IZCOZ0_182967/1
Swiss National Science Foundation (SNF)
Wildhainweg 3, CH-3001 Berne
www.snf.ch

Subsidy recipients:
Scuola universitaria professionale della Svizzera italiana (SUPSI)
Campus Mendrisio, Via Flora Ruchat-Roncati 15, CH-6850 Mendrisio
www.supsi.ch

Authors:
Ebrar Özkalay, SUPSI, ebrar.oezkalay@supsi.ch

SFOE project coordinators:
Stefan Oberholzer, Swiss Federal Office of Energy, stefan.oberholzer@bfe.admin.ch
SFOE contract number: SI/501982-01

Summary

One of the important applications of PV energy is building integrated photovoltaic (BIPV) systems, which transform building envelopes into power plants while keeping the building properties such as thermal isolation, water-tightness, shading, etc. PV manufacturers provide 25 years of warranty for the PV modules. However, there is a trend towards 30-35+ years of a lifetime for properly produced modules. BIPV modules could experience somehow harsher operating conditions compared to field-deployed PV modules. Nevertheless, BIPV products are expected to have long service lifetimes since other building components generally have lifetimes targeting 40 years. By improving the reliability and durability of BIPV products, thus its lifetime, BIPV could be more appealing and cost-effective for building owners, installers and architects. This research project aims to assess and improve the reliability and long-term performance of BIPV modules and systems. This is done by; 1) Analysing long-term performance data from a statistically representative number of BIPV systems and mock-up structures to assess the impact of specific operating conditions on degradation rates of BIPV modules, and 2) Performing indoor and outdoor accelerated ageing tests to address specific failure modes that BIPV modules experience.

In this work, we show that there may be larger thermal and thermo-mechanical stresses in BIPV operating conditions which may accelerates some degradation mechanisms such as UV-induced degradation (discoloration and loss in Isc) or causes issues on metallization (loss in FF). Additionally, PV modules may have issues originated from their production, e.g., encapsulant material susceptible to UV and thermal stresses. Those issues could not be important for the safety and performance of conventional PV; however, for BIPV applications, imperfect production could be more significant since the operating conditions are more challenging than conventional PV. However, modules operating in a BIPV configuration do not have to degrade faster. There could be faster degradation only if there are larger thermal and-or thermo-mechanical stresses (except repetitive shadow stress). As shown in this work, for example if a ventilation chamber of a BIPV-ventilated module is well designed, there will not be high thermal and thermo-mechanical stresses and accelerated degradation mechanisms due to those additional stresses.

Zusammenfassung

Eine der wichtigsten Anwendungen der Photovoltaik sind gebäudeintegrierte PV-Anlagen (BIPV), die Gebäudehüllen in Kraftwerke umwandeln und dabei die Gebäudeeigenschaften wie Wärmeisolierung, Wasserdichtigkeit, Beschattung usw. beibehalten. PV-Hersteller gewähren 25 Jahre Garantie auf die PV-Module. Es gibt jedoch einen Trend zu einer Lebensdauer von mehr als 30-35 Jahren. BIPV-Module können im Vergleich zu in Freiflächen eingesetzten PV-Modulen härteren Betriebsbedingungen ausgesetzt sein. Dennoch wird erwartet, dass BIPV-Produkte eine lange Lebensdauer haben, da andere Bauteile im Allgemeinen eine Lebensdauer von 40 Jahren haben. Durch die Verbesserung der Zuverlässigkeit und Beständigkeit von BIPV-Produkten und damit ihrer Lebensdauer könnte BIPV für Bauherren, Installateure und Architekten attraktiver und kostengünstiger werden. Das Hauptziel dieses Forschungsprojekts ist die Bewertung und Verbesserung der Zuverlässigkeit und Leistungsbeständigkeit von BIPV-Modulen und -Systemen. Dies wird erzielt durch; 1) Analyse von Langzeitleistungsdaten einer statistisch repräsentativen Anzahl von BIPV-Systemen und Teststänđen, um die Auswirkungen bestimmter Betriebsbedingungen auf die Degradationsrate von BIPV-Modulen zu bewerten, und 2) Entwerfen von Tests zur beschleunigten Alterung, um bestimmte Fehlermechanismen zu untersuchen, die bei BIPV-Modulen auftreten.

In dieser Arbeit zeigen wir, dass es unter BIPV-Betriebsbedingungen zu größeren thermischen und thermomechanischen Belastungen kommen kann, die einige Degradationsmechanismen wie UV-induzierte Degradation (Verfärbung und Isc-Verlust) beschleunigen oder Probleme bei der Metallisierung (FF-Verlust) verursachen können. Darüber hinaus können PV-Module Probleme aufweisen, die auf ihre Herstellung zurückzuführen sind, z. B. Verkapselungsmaterial, das anfällig für

UV- und thermische Belastungen ist. Diese Probleme könnten für die Sicherheit und Leistung konventioneller PV nicht von Bedeutung sein; bei BIPV-Anwendungen könnte eine mangelhafte Produktion jedoch von größerer Bedeutung sein, da die Betriebsbedingungen schwieriger sind als bei konventioneller PV. Module, die in einer BIPV-Konfiguration betrieben werden, müssen jedoch nicht schneller degradieren. Eine schnellere Degradation könnte nur dann eintreten, wenn größere thermische und/oder thermomechanische Belastungen auftreten (mit Ausnahme der wiederholten Schattenbelastung). Wie in dieser Arbeit gezeigt wurde, kommt es beispielsweise bei einer gut konzipierten Belüftungskammer eines BIPV-belüfteten Moduls nicht zu hohen thermischen und thermomechanischen Spannungen und beschleunigten Degradationsmechanismen aufgrund dieser zusätzlichen Spannungen.

Contents

Abbreviations

BAPV	Building Applied Photovoltaics
BIPV	Building Integrated Photovoltaics
BS	Backsheet
CO_2	Carbon dioxide
EL	Electroluminescence
EVA	Ethylene-vinyl acetate
FF	Fill factor
G_{POA}	Plane of array irradiance
GW	Gigawatt
HJT	Heterojunction cell technology
IBC	Integrated back contact
IEC	International Electrotechnical Commission
I_{sc}	Short-circuit current
IV	Current-Voltage
LCOE	Levelised cost of energy
MQT	Module quality test
PERC	Passivated Emitter and Rear Cell
PID	Potential induced degradation
PR	Performance ratio
PR_{cor}	Temperature corrected performance ratio
PV	Photovoltaics
PVB	Polyvinyl butyral
ROI	Return of investment
STC	Standard test condition
STL	Seasonal and trend decomposition with LOESS
T_{98}	98th percentile temperature
T_{max}	Maximum module operating temperature
TS	Technical standard
TWh	Terawatt-hour
USD	United States dollar
UTC	Coordinated Universal Time
UV	Ultraviolet
VI	Visual inspection
V_{oc}	Open-circuit voltage
WL	Wet-leakage
YoY	Year-over-Year

1 Introduction

The Swiss National Science Foundation (SNF), which partially funded this project, has given an additional year for the successful completion of the project in accordance with the proposal. This extension was granted due to completing 4 years of PhD study and the long delays of some tasks due to Covid-related reasons. While there was a delay in the tasks of WP2 and WP3, WP1–Task 2 was extended with analyses of historical data to compensate for the unavailability of project data. For this reason, deliverable 1.4 (Evaluation of Long-term Performance Analysis Methods and Satellite-derived Insolation data for the long-term analysis, and long-term Performance Analysis of historic/existing data) is added to the project. The methodologies that have been used in these analyses were not mentioned in the initial research plan. Some in-depth research and analysis have been presented at some conferences or published as peer-reviewed articles. The methods used in these analyses will be used to analyze the data from the installed test stands within this or other projects. There are few studies still ongoing, for example, detailed long-term performance analysis of existing BIPV test stands (SUPSI's historical data) and uncertainty analysis of performance ratio (PR) and performance loss rate (PLR) using ground and satellite-derived insolation data. We can say that Covid-19-related delays were compensated strongly by data analysis and long-term data analysis of historical data.

1.1 Background information and current situation

Solar photovoltaic (PV) is one of the most promising renewable energy technologies. Since its start in the late 1990s, total PV deployment has dramatically increased, with the first terawatt built at the beginning of 2022 [1]. PV contributes to more than 3.7% of annual global electricity demand and 6% in Europe [2]. By 2050, cumulative installed PV and wind energy together are projected to provide 60% of global electricity generation [3]. An important driver of globally increasing PV capacity is the downward trend in crystalline silicon (c-Si) PV module costs, which declined by 90% from 2009 to 2019 reaching prices close to 0.27 USD/W [4]. Cost reductions are related to various factors: improvements in polysilicon production, cell and module efficiency, and manufacturing (e.g., diamond-wire sawing). In addition, a decrease in the cost of balance of system (BoS), more experienced project developers and supply chain structures lead to a decline in the cost of PV installation. Cost reductions in PV modules and BoS (less steeply compared to PV modules) have driven reductions in the globally weighted levelised cost of energy (LCOE) and reached 0.057 USD/kWh in 2020 [3]. Since 2014, the globally weighted LCOE of solar PV is into the range of fossil fuels (sometimes it is even lower); thus, PV has started to compete directly with fossil fuels with continued cost reductions [5].

"Energy Strategy 2050" is Switzerland's new energy policy and aims to restructure the energy system of Switzerland, including increasing the use of renewable energy and reducing energy-related CO_2 emissions. Today, PV contributes around 52% to renewable electricity production (excluding hydropower), and contribution, in particular, has grown enormously since 2010 [6]. However, in countries like Switzerland, land availability for ground PV installations is a challenge on the spread of PV installations. Therefore, building surfaces, which have an estimated 67 TWh annual electricity potential in Switzerland [7], will have to host PV in order to reach future energy goals. Today, residential and commercial buildings are responsible for about 40% of the global energy demand and 25% of the total CO_2 generation [8]. Building Integrated Photovoltaics (BIPV) is one of the most efficient ways to reduce CO_2 emission and generate own electricity for nearly zero energy buildings by saving in terms of energy and construction cost [9, 10, 11]. Besides electricity generation, BIPV modules are multifunctional; they provide thermal insulation, noise protection, weather protection, etc. Nevertheless, BIPV market is still a niche market, about 1-2% of the global PV market, with a considerable growth potential thanks to decreasing cost of PV and demanding legislations for high-performance buildings [8, 12].

As opposed to the majority of rooftop PV installations, where the modules are added on top of an existing building element (e.g., roof), BIPV modules/systems are part of the building envelope. BIPV elements are therefore "building active elements" that generate electricity while simultaneously providing

building envelope functions, such as weather protection (waterproofing, sunshade), thermal insulation, noise protection, daylight illumination or safety. The main difference between building applied PV (BAPV) and BIPV is the multi-functionality of BIPV besides electricity generation. BIPV has been proven to be important in implementing nearly zero-energy buildings since it can produce clean electricity close to the end user, minimising land use [13]. Furthermore, BIPV is a building material that has interesting return of investment (ROI) relative to non-PV building materials [14]. Currently, the BIPV market holds about 2% of the overall PV market. The analyses estimate rapid growth in BIPV penetration due to legislations of the European Union on near-zero energy buildings and a decrease in the cost of PV [15, 16]. The main application areas of BIPV are roofs (e.g., full-roof, in-roof, solar tiles, skylights), façades (e.g., curtain wall, rain screen façade, windows) and external systems (e.g., balcony railings, shadings). Some examples of BIPV systems are shown in Figure 1 together with a typical BAPV installation. BIPV modules are installed in three different configurations on façades and roofs which are insulated (restricted air ventilation at rear side of module), ventilated (reduced air ventilation at air gap between module and building) and open-rack (full air ventilation, e.g., balcony railings).

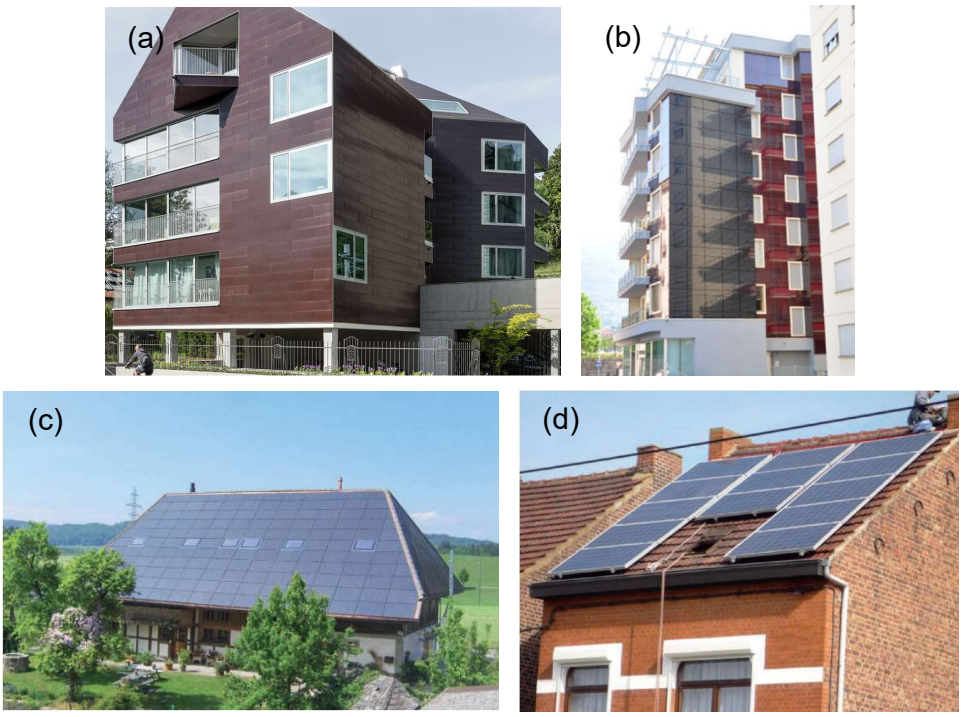

Figure 1: (a) Coloured BIPV modules on façade and roof. Image is taken from [17]. (b) Palazzo Positivo: Coloured c-Si modules as rain screen façade [18]. (c) Full-roof BIPV installation. Image is taken from [19]. (d) Typical BAPV installation. Image is taken from [19].

With the increasing adoption of PV in the residential market, some barriers still need to be solved to ensure the implementation of cost-effective solutions for BIPV as opposed to passive/conventional building components. One crucial thematic is the products' reliability and long-term performance that involves producing electricity for 30-40 years and keeping building properties through time, such as safety, durability, and comfort. Conventional PV modules mostly have 20-25 years of performance warranty, whereas traditional building elements often preserve their mechanical stability and safety for 40+ years. Unlike conventional field installations, BIPV modules are generally not installed at an optimal orientation or conditions. Furthermore, BIPV modules could be exposed to more challenging operating conditions. The most common harsher operating conditions of the BIPV modules relative to field-installed PV are:

1) Operating at higher temperatures due to reduced or restricted ventilation [20, 21],

2) Higher diurnal (including night-time) temperature changes [22] and

3) Periodic shading caused by surrounding buildings or other obstacles.

The aforementioned operating conditions have an impact on the performance as well as reliability and durability of BIPV modules. These conditions push the limits of cell interconnections, cell and module packaging materials (encapsulant, front and back cover). There are various performance losses causing failure modes observed in a field, such as delamination between packaging layers, hot-spots, interconnect failures, discolouration of encapsulant and backsheet foil, glass breakage, potential induced degradation (PID) [23]. Those failure modes could be accelerated at BIPV operating conditions. Since BIPV modules are part of an urban environment, deterioration of electrical insulation or broken glass eventually leads to safety issues. However, these operating conditions depend on the application type. For example, the BIPV module with an insulated backside on a roof has more thermal stress than the BIPV module as a rain screen façade application with ventilation.

1.2 Purpose of the project

Expertise and knowledge about the reliability of BIPV panels/systems is often limited and is mostly qualitative rather than quantitative. A deeper understanding of the performance degradation during real-world operation is critical to predicting a PV system's long-term reliability. Therefore, analysis of the long-term performance of monitored BIPV systems is crucial. Further, when considering the specific (and more challenging) operating conditions of BIPV devices, understanding the additional ageing contributions (compared to field-mounted devices) is of paramount importance. The project aims to investigate the operating conditions and additional ageing contributions of c-Si BIPV modules to increase the adoption of this technology in the built environment and learn more about how to test and prevent additional accelerated degradation modes of BIPV modules.

1.3 Objectives

The primary goal of this research work is to assess and improve the reliability and long-term performance of BIPV modules and systems. This goal is divided into two research questions:

1. Do the specific mounting configurations and operating conditions of BIPV modules impact their long-term performance and degradation rates (quantitative versus qualitative assessment)? We will reply to these specific questions by:
    a. Analysing long-term monitored data from existing BIPV mock-up structures.
    b. Collecting long-term data from statistically representative samples of BIPV modules/installations (with different mounting configurations and degrees of shading) and comparing the long-term degradation rates.
2. How to improve the BIPV modules' testing to improve their reliability and long-term performance? We will reply to this question by:
    a. Analysing the modules from the BIPV mock-ups and systems that were investigated, in order to detect specific failure modes that can be ascribed to the specific operating conditions of BIPV modules.
    b. Improving the current accelerated-ageing tests in order to address these specific BIPV failure modes and complement the conventionally adopted industry qualification standards.
    c. Designing and installing new outdoor test stands for integrating and monitoring new BIPV module concepts presently entering the market.

2 Procedures and methodology

Field assessment of reliability issues linked to BIPV is significant in order to solve one of the crucial barriers in front of BIPV applications. The first activity is the investigation of performance degradation rates of BIPV systems and modules depending on the operating condition. Long-term data from the BIPV mock-ups and BIPV buildings that we are monitoring are used in the analysis. More field data are collected in order to expand our database and the statistical relevance of our analysis. In this way, impact of operating condition on long-term performance of BIPV modules is investigated and the degradation modes triggered by those conditions can be analysed.

Findings from the long-term performance analysis of BIPV modules and systems are utilised to make necessary changes to the testing condition of BIPV related indoor reliability tests in the IEC 61215-2 to mimic BIPV operating conditions and related failure mechanisms. The BIPV related indoor reliability tests are executed in standard and proposed (beyond the standard) test conditions.

The BIPV modules, which were already installed at SUPSI, have been installed again in BIPV condition in order to longer the duration of outdoor exposure (beyond 4 years). In addition, a set of four different PV products were procured based upon the PV market projections and BIPV needs. They have been installed in open-rack and BIPV conditions. Since the project's duration is not long enough to detect performance degradation of PV modules (if the modules are well manufactured), modules have been installed to the outdoor test stand with additional stresses to trigger and accelerate degradation and failure modes. The additional stresses are created by using heat blankets and shadow masks separately. The monitoring of the mock-ups is on-going since May-2022.

3 Activities and results

3.1 Work Package 1: Reference Framework

This section presents the progress on Work Package 1 (reference framework) of the project. Except Task 2, all other Tasks (1, 3 and 4) are finished. In section 3.1.1 (Task 1), BIPV modules and their technologies were reported. Then, type of installed BIPV products on the 211 BIPV systems in Europe has shown. In section 3.1.2 (Task 2), operating conditions of various BIPV systems (in-roof, cold-façade) has been reported. Further, the impact of the BIPV operating condition on the long-term performance has been presented (Section 3.1.3). In this way, limit conditions of various BIPV configurations have been understood. The information from this task have been used to define outdoor mock-ups and indoor qualification/reliability tests for BIPV modules. This is explained in section 3.2.2. Task 2 is intentionally still ongoing since there is a lack of accurate BIPV data analysis, which is important for reliability studies of BIPV modules. As part of Task 2, section 3.1.4, quantitative analysis on performance loss rate analysis using satellite versus ground meteorological data is presented, and section 3.1.5, uncertainty of satellite-derived insolation data and performance ratio computed using satellite insolation data is presented.

3.1.1 BIPV modules and Structures on the Market

Initially, BIPV modules and structures in the market were analyzed. Roof products have the largest share in BIPV market by around 60% against façade products (external systems included in façade products) [24]. Full-roof and in-roof solutions, and solar tiles are the main roof products (26% and 24%, respectively) while for façades, cold-façade BIPV products have the largest share by 13% of total market. However, it must be noted that many BIPV systems have custom designed products that are not offered in the market. Moreover, the market changes quickly while some companies stop their production, others enter to the market with new products [25]. In the market, c-Si cell technology is preferred for roof products by 72% due to its higher efficiency relative to thin film. However, for façade

products, thin film technology have 44% share while c-Si have 34%, which could be explained by lower cost and better aesthetics (colored) of thin film modules. In addition, it has been seen that mainly roof products were preferred (more than 70% of 211 installations in Europe) but it must be noted that this is limited to the number of BIPV systems that were analyzed.

3.1.2 Operating Temperatures of the BIPV Modules

Considering the lack of long-term BIPV performance data by using properly maintained/calibrated irradiance and module temperature sensors with high-frequency sampling, analyses of long-term outdoor performance of BIPV modules is crucial to understand the theoretical limits and operating conditions of BIPV modules. Three BIPV outdoor test stands were monitored at SUPSI in Canobbio, Switzerland, which according to the Köppen-Geiger is classified as Cfb climate zone (temperate and humid climate, and warm summers). Modules on the test stands were installed in open-rack and various BIPV configurations as summarised in Figure 2 and **Errore. L'origine riferimento non è stata trovata.**. Open-rack configuration is the most common and conventional PV module installation configuration, and modules in this configuration are expected to operate at lower temperatures compared to modules in BIPV configurations due to free ventilation on the rear-side of module. Full-roof, in-roof and cold-façade BIPV configurations are the most common BIPV configurations and they could have ventilation chamber between module and insulation layer, which ensures partial ventilation on the rear-side of the module as shown in Figure 2. In this work, the modules in this configuration are referred to as BIPV-Ventilated modules. The last BIPV configuration is the insulated configuration where there is no gap between module and insulation layer. Hence, there is no ventilation at the rear-side of module. In this work, modules in this configuration are referred to as BIPV-Insulated module. The heterojunction technology (HJT) modules on Test Stand-2 are prototype modules while the other modules are commercial products.

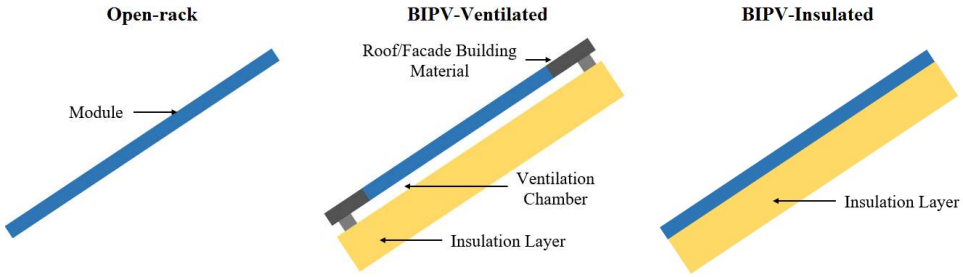

Figure 2: Summary of installation configurations on the BIPV test stands.

Table 1: Types of the modules from the outdoor test stands together with their installation configuration, azimuth and tilt angles, outdoor deployment duration, monitored parameters and their time resolution.

Test Stand	Cell and Module Technologies	Installation Configuration	Azimuth (North = 0˚) / Tilt Angles	Duration	Monitored Parameters
1	Al-BSF - G/EVA/BS Commercial module	• Open-rack • BIPV-Insulated	176˚ / 6˚ (Roof)	51 Months	• G_{POA} (every 1 minute) • Module Temperature (Pt100 on rear-side of modules) (every 1 minute) • IV curves (every 5 minutes)
	Al-BSF - G/PVB/G Commercial module				
2	HJT - G/G Prototype module	• Open-rack • BIPV-Ventilated	176˚ / 20˚ (Roof)	53 Months	
	PERC - G/EVA/BS Commercial module	• BIPV-Ventilated			
3	PERC - G/PVB/G Commercial module	• BIPV-Ventilated	176˚ / 90˚ (Façade)	27 Months	

Al-BSF: Aluminum back surface field, HJT: Heterojunction Technology, PERC: Passivated Emitter and Rear Contact, G: Glass, BS: Backsheet, EVA: Ethylene-vinyl acetate, PVB: Polyvinyl-butyral and G_{POA}: Plane of array irradiance.

Recently, the International Electrotechnical Commission (IEC) published a technical specification (TS) called IEC TS 63126 “Guidelines for qualifying PV modules, components and materials for operation at high temperatures” [26] since some modules in hot climates or in BIPV configurations may operate at temperatures higher than those used in the qualification and safety tests of IEC 61215 and 61730 [27, 28]. The TS suggests two new testing conditions for the related indoor qualification and safety tests depending on the 98th percentile operating module temperature (T_{98}) (Level 1 Test Condition for 70˚C < T_{98} ≤ 80˚C and Level 2 Test Condition for 80˚C < T_{98} ≤ 90˚C). T_{98} represents combination of a cumulative exposure of 175.2 hours/year at or above the stated temperature. However, there is lack of analysis on operating module temperature in BIPV configurations.

Operating temperature distributions of the modules on the test stands for the duration of their monitoring periods are shown in Figure 3 and summarised in As shown in various studies , exposure of the modules to elevated operating temperatures may lead to higher degradation rates (e.g., higher rate of encapsulant discoloration, damaged interconnections and solder joints, etc.) and a faster occurrence of wear-out-failures that shorten the lifetime of a PV module.

. The insulated modules in Test Stand-1 operated at higher temperatures due to absence of rear-side ventilation (Figure 3a). While the open-rack modules reached a maximum of 62˚C and 66˚C, respectively, the insulated modules exhibited a larger distribution, reaching temperatures slightly above 90˚C. T_{98} of the insulated modules in Test Stand-1 are 80˚C, while T_{98} of the open-rack G/BS and G/G modules are 57˚C and 53˚C, respectively (As shown in various studies , exposure of the modules to elevated operating temperatures may lead to higher degradation rates (e.g., higher rate of encapsulant discoloration, damaged interconnections and solder joints, etc.) and a faster occurrence of wear-out-failures that shorten the lifetime of a PV module.

). Interestingly, the insulated modules are exposed to lower temperatures (even below 0˚C) with respect to modules in open-rack conditions. This is due to the stronger radiative cooling for the insulated modules compared to the open-rack modules at night. This behaviour has been observed by others [29] [30].

In Test Stand-2, the ventilated HJT module reached higher operating temperatures than the same module type in open-rack configuration due to limited rear-side ventilation (Figure 3b). T_{98} of the open-rack and the ventilated HJT modules are 50˚C and 71˚C, respectively (As shown in various studies , exposure of the modules to elevated operating temperatures may lead to higher degradation rates (e.g., higher rate of encapsulant discoloration, damaged interconnections and solder joints, etc.) and a faster occurrence of wear-out-failures that shorten the lifetime of a PV module.

). The ventilated PERC module has a T_{98} of 63˚C (maximum of 77˚C). In the ventilated roof configuration, the HJT module operated warmer than the PERC module, which could be due to difference in the design of the ventilation systems (e.g., different ventilation chamber thicknesses and techniques, and ventilation outlet positions), the position of the module within the roof surface and parasitic absorption by transparent conductive oxide (TCO) layer of the HJT cells [31].

The ventilated G/G PERC BIPV module, installed as a ventilated façade module on Test Stand-3, operated at lower temperatures as compared to the other modules in BIPV configurations (Figure 3c). As expected, this is due to the fact that façades received a higher insolation in winter months (e.g., when the sun is lower on the horizon, and average temperatures are lower) with respect to summer months. On the contrary, the modules on a sloped surface generally reach their maximum operating temperatures in summer when solar altitude and ambient temperatures are high.

Table 2: Maximum temperature (T_{max}) and T_{98} of the modules from Test Stand-1, Test Stand-2 and Test Stand-3. T_{98} values, which are high enough to propose harsher testing conditions for the related tests according to IEC TS 63126 [26], are in bold.

Test Stand	Cell and Module Technologies	Tilt Angles	Open-Rack		BIPV-Ventilated		BIPV-Insulated	
			T_{98} [˚C]	T_{max} [˚C]	T_{98} [˚C]	T_{max} [˚C]	T_{98} [˚C]	T_{max} [˚C]

1	Al-BSF - G/EVA/BS	6˚	57	66	-	-	**80**	92
	Al-BSF - G/PVB/G	6˚	53	62	-	-	**80**	91
2	HJT - G/BS	30˚	50	64	**71**	83	-	-
	PERC - G/EVA/BS	30˚	-	-	63	77	-	-
3	PERC - G/PVB/G	90˚	-	-	59	68	-	-

T_{98} of the two insulated BIPV modules on Test Stand-1 and the ventilated HJT module on Test Stand-2 are all higher than 70˚C, as shown in As shown in various studies , exposure of the modules to elevated operating temperatures may lead to higher degradation rates (e.g., higher rate of encapsulant discoloration, damaged interconnections and solder joints, etc.) and a faster occurrence of wear-out-failures that shorten the lifetime of a PV module.

. According to the IEC TS 63126, these modules should be tested at harsher testing conditions in a selection of indoor module qualification and safety tests defined in IEC 61215 and IEC 61730. As shown in various studies [32, 33, 34], exposure of the modules to elevated operating temperatures may lead to higher degradation rates (e.g., higher rate of encapsulant discoloration, damaged interconnections and solder joints, etc.) and a faster occurrence of wear-out-failures that shorten the lifetime of a PV module.

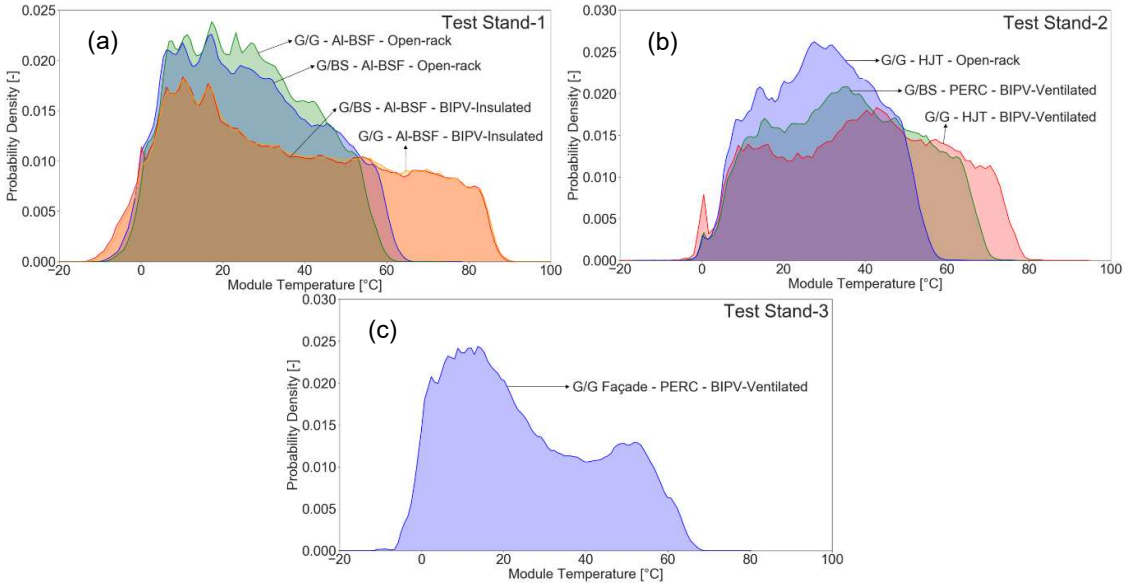

Figure 3: Temperature distribution of the modules from (a) Test Stand-1, (b) Test Stand-2 and (c) Test Stand-3 during their outdoor deployment.

Another harsher operating condition for BIPV modules compared to open-rack PV is the larger diurnal module temperature change (including night-time). Diurnal temperature changes (ΔT_D) were calculated from the difference between maximum and minimum module temperature in a day. Figure 4 shows the distribution of diurnal temperature changes of the modules in Test Stand-1, Test-Stand-2 and Test Stand-3. The slight increase in the probability density of ΔT_D below 15˚C is due to overcast and cloudy days. For cloudy days, the median of ΔT_D distributions ($\Delta T_{D,med}$) of the modules are between 10 to 13˚C, and there is no significant difference between the modules since the amount of received irradiance is low. The higher probability densities of ΔT_D above 20˚C represent clear sky days. Depending on the various parameters (e.g., mounting configuration, module technology, inclination), the peak of ΔT_D distribution differs between the modules (Figure 4).

In Test Stand-1, the $\Delta T_{D,med}$ of the open-rack modules are around 26 to 30˚C, while the $\Delta T_{D,med}$ of the insulated modules are around 50 to 51˚C (Table 3). For the G/G modules, the $\Delta T_{D,med}$ of the insulated

module (51˚C) is almost twice as the $\Delta T_{D,med}$ of the open-rack module (26˚C). The maximum ΔT ($\Delta T_{D,max}$) for the insulated modules reached 76 to 77˚C, while for the open-rack modules, it was never above 50˚C.

In Test Stand-2, although the $\Delta T_{D,med}$ of the open-rack HJT module is 26˚C, the ventilated HJT module has the median at 44˚C (Table 3). The $\Delta T_{D,max}$ of the ventilated HJT and PERC roof modules are 66˚C and 58˚C, respectively. Since the ventilated HJT BIPV module ran warmer than the ventilated PERC BIPV module, it was exposed to greater ΔT_D. The insulated G/G BIPV module on Test Stand-1 was exhibited a greater ΔT_D compared to the ventilated G/G HJT BIPV module on Test Stand-2 (Figure 4a and Figure 4b). This is mainly because the insulated configuration has no rear-side ventilation, whereas the ventilated configuration has limited rear-side ventilation.

As shown in As shown in various studies , exposure of the modules to elevated operating temperatures may lead to higher degradation rates (e.g., higher rate of encapsulant discoloration, damaged interconnections and solder joints, etc.) and a faster occurrence of wear-out-failures that shorten the lifetime of a PV module.

, there is no significant difference between the T_{98} and the maximum temperatures of the open-rack modules (Test Stand-1 and 2) and the ventilated façade module on Test Stand-3. On the other hand, the façade module experienced higher ΔT_D than the open-rack modules (Figure 4). The $\Delta T_{D,med}$ of the ventilated façade module on Test Stand-3 is 43˚C, which is well above the $\Delta T_{D,med}$ of any open-rack module (13 to 17˚C more) as shown in Table 3.

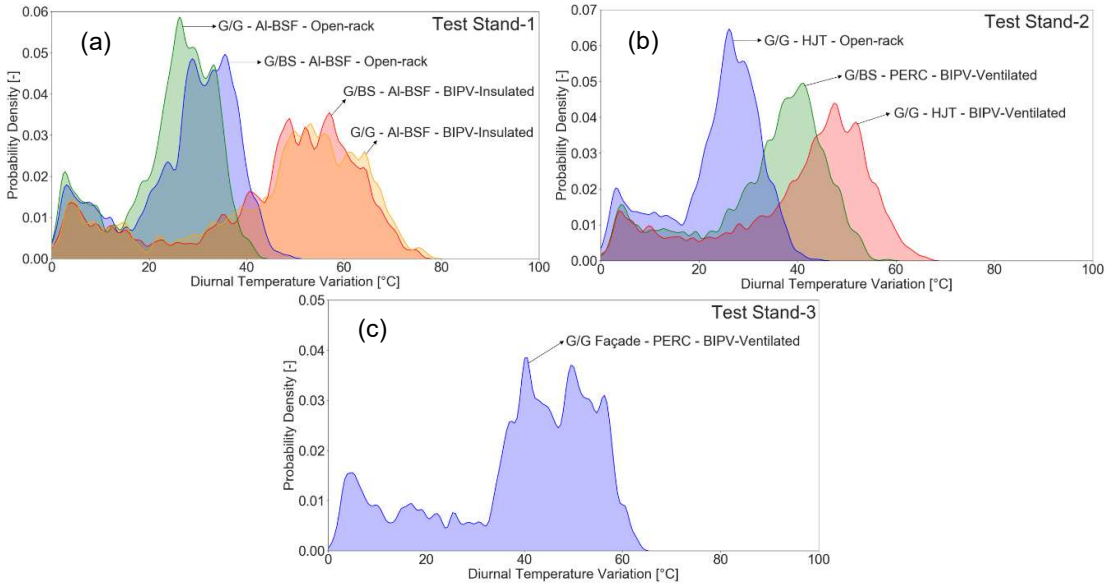

Figure 4: Diurnal temperature change (ΔT_D) distribution of the modules from (a) Test Stand-1 and (b) Test Stand-2. Temperature measurements are between 4:00 AM and 9:00 PM. All times are Coordinated Universal Time (UTC).

Table 3: Median ($\Delta T_{D,med}$) and maximum ($\Delta T_{D,max}$) diurnal temperature variations of the modules from Test Stand-1, Test Stand-2 and Test Stand-3.

Test Stand	Cell and Module Technologies	Tilt	Open-Rack		BIPV-Ventilated		BIPV-Insulated		Difference (BIPV – Open-rack)	
			$\Delta T_{D,med}$ [˚C]	$\Delta T_{D,max}$ [˚C]	$\Delta T_{D,med}$ [˚C]	$\Delta T_{D,max}$ [˚C]	$\Delta T_{D,med}$ [˚C]	$\Delta T_{D,max}$ [˚C]	**$\Delta T_{D,med}$ [˚C]**	**$\Delta T_{D,max}$ [˚C]**
1	Al-BSF - G/EVA/BS	6˚	30	49	-	-	50	76	**20**	**27**
	Al-BSF - G/PVB/G	6˚	26	42	-	-	51	77	**25**	**35**
2	HJT - G/G	20˚	26	44	44	66	-	-	**18**	**22**

	PERC - G/EVA/BS	20˚	-	-	37	58	-	-	-	-
3	PERC - G/PVB/G	90˚	-	-	43	63	-	-	-	-

Even in a vertical façade, BIPV modules were exposed to larger ΔT_D than the corresponding modules mounted in an open rack configuration. Figure 5 shows the plane of array irradiances and module temperatures from Test Stand-2 and Test Stand-3 on December 24, 2017, the closest clear sky day to the winter solstice. When the sun is low on the horizon, the vertical façade module on Test Stand-3 has higher operating temperatures than the 20°-tilted roof modules on Test Stand-2, because of the higher amount of irradiance received. Hence, the façade BIPV module has higher ΔT_D (59°C) with respect to the other modules (maximum of 49°C). The façade module experienced the $\Delta T_{D,max}$ in clear-sky days when the solar altitude was low compared to June, and the night-time temperatures were frequently below 5°C, especially around late February, March, and early April for Canobbio. The sloped modules experienced the $\Delta T_{D,max}$ in clear-sky days when the differences between day and night ambient temperatures were high (>13°C), and the solar altitude was higher compared to December, especially around late March, April, August, and September for Canobbio. The time of the year with the $\Delta T_{D,max}$ could slightly vary depending on the tilt of the sloped modules.

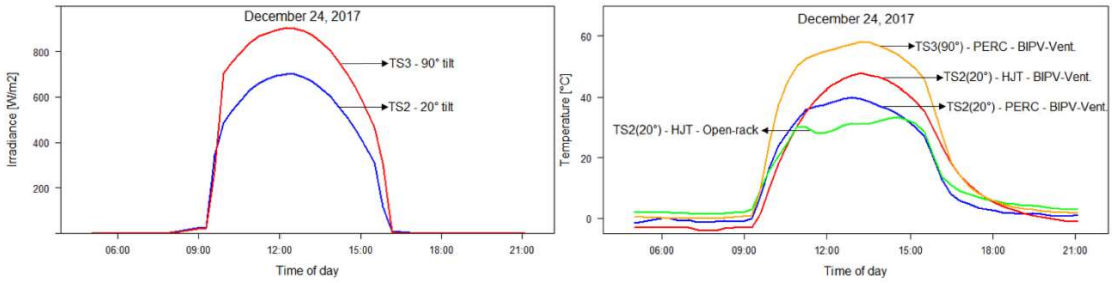

Figure 5: (left) Daily plane of array irradiance and (right) module temperature profiles from Test Stand-2 (TS2) (20° tilt) and Test Stand-3 (TS3) (90° tilt) on December 24, 2017, the closest clear sky day to the winter solstice. All times are local time (UTC+1).

Larger temperature changes increase thermo-mechanical stresses on interconnects and cells due mismatches in the thermal expansion coefficients of the different materials used in the module sandwich [35]. Modules exposed to larger thermo-mechanical stresses may more easily be prone to larger failure rates of solder joints, interconnects or cells. Over an extended period, these degradation mechanisms may cause current mismatches between cells (evolving in other defects and in the worst case leading to hot-spot generation), increase in module's series resistance, and eventually in loss of power [36]. Various studies [37, 38] have demonstrated that modules in hot climates are subject to larger power losses due to increased series resistance compared to modules in cold climates. Increased series resistance could be one of the possible mechanisms for larger degradation rates of the modules operating at elevated temperatures. Furthermore, cell and metallisation defects could cause hot spot and enhance occurrence of other failure modes such as discoloration, glass breakage and loss of electrical insulation.

Due to the exposure to higher operating temperatures, diurnal temperature changes, and proximity to end-users in buildings, BIPV modules should satisfy stricter safety and performance requirements (IEC TS 63126, IEC 63092-1, IEC 63092-2 and other regional and national standards specific to building materials), which can lead to modifications of the qualification and safety indoor tests. More detailed information on this study can be found in [39].

3.1.3 Long-term Performance of the BIPV Modules

Long-term performance analysis of the modules mentioned in the previous subsection is still ongoing. Table 4 shows the long-term performance analysis of the modules (Test Stand-1, Test Stand-2 and Test Stand-3). We see that since larger thermal stress accelerates UV-induced degradation of EVA, there could be loss in I_{sc} in BIPV configurations. In addition, due to larger thermo-mechanical

stress, there could be damaged cells and metallization that cause FF loss (Test Stand-1, Al-BSF G/EVA/BS module). In addition, PV modules may have issues originated from their production, e.g., encapsulant material susceptible to UV and thermal stresses. In this case, the results from Test Stand-2 (c-Si, G/G, BIPV-ventilated prototype module) show that those issues could not be important for the safety and performance of conventional PV; however, for BIPV applications, imperfect production could be more significant since the operating conditions are more challenging than conventional PV.

In addition to the long-term performance analysis using outdoor monitored data, performance of the modules at STC were measured before and after outdoor exposure (Table 5). Moreover, non-destructive material analysis (Raman, FTIR, UV-VIS, NIR spectrums, and UV-Fluorescence imaging) was performed on the modules from Test Stand-1 and Test Stand-2 at OFI, Austria under COST PEARLPV. Currently, we are analysing all the data we have for these modules and finding correlations between different analysis methods (outdoor data, indoor electrical characterisation and non-destructive material characterisation). Results from outdoor data analysis (PLR), indoor measurements and material characterisation will be merged and a manuscript will be written on long term performance of SUPSI's historic BIPV test stands in early 2023.

Table 4: Performance loss rates (PLR) of PR and IV parameters of the modules on Test Stand-1, Test Stand-2 and Test Stand-3 by applying averaging PLRs method in [40].

	Test Stand-1				**Test Stand-2**			**Test Stand-3**
Module Tech.	**Al-BSF - G/EVA/BS**		**Al-BSF - G/PVB/G**		**HJT – G/G Prototype Module**		**PERC - G/EVA/BS**	**PERC – G/EVA/BS**
Mounting Configuration	**Open-rack**	**BIPV-Insulated**	**Open-rack**	**BIPV-Insulated**	**Open-rack**	**BIPV-Ventilated**	**BIPV-Ventilated**	**BIPV-Ventilated (façade)**
PR [%/yr]	-0.03	-0.33	-0.05	0.25	-0.83	-1.83	-0.01	-0.02
Isc [%/yr]	-0.09	-0.03	-0.04	0.48	-0.28	-0.97	-0.10	-0.04
Voc [%/yr]	0.03	-0.07	-0.07	0.03	-0.11	-0.01	-0.06	0.02
FF [%/yr]	0.03	-0.29	0.01	-0.15	-0.51	-0.81	0.07	-0.01

Table 5: Change between the initial and final indoor IV measurements of the modules on Test Stand-1, Test Stand-2 and Test Stand-3.

	Test Stand-1				**Test Stand-2**			**Test Stand-3**
Module Tech.	**Al-BSF - G/EVA/BS**		**Al-BSF - G/PVB/G**		**HJT – G/G Prototype Module**		**PERC - G/EVA/BS**	**PERC – G/EVA/BS**
Mounting Configuration	**Open-rack**	**BIPV-Insulated**	**Open-rack**	**BIPV-Insulated**	**Open-rack**	**BIPV-Ventilated**	**BIPV-Ventilated**	**BIPV-Ventilated (façade)**
ΔPm [%]	-0.3	-3	-1.7	-1.9	-4.4	-11.6	-0.8	0.01
ΔIsc [%]	0.1	-0.9	-1.7	-1.7	-2.7	-6.2	-0.4	0.07
ΔVoc [%]	0.2	-0.3	-0.05	-0.15	-0.1	-0.2	0.2	0.2
ΔFF [%]	-0.5	-1.6	0.1	-0.1	-1.5	-0.81	-0.7	-0.26

3.1.4 Quantifying Performance Loss Rates of Photovoltaic Modules using Ground-based vs Satellite-based Meteorological Data

Accurate assessment of the long-term performance of PV systems is critical for manufacturers, investors, plant owners and O&M companies. Many PV systems, especially residential and some commercial/industrial systems are not equipped with meteorological monitoring systems such as irradiance and temperature sensors. Whereas to calculate the performance ratio (PR), a common performance measure, the plane of array irradiance (G_{POA}) is an input parameter. The irradiance data is the largest contribution to uncertainty in PR. Therefore, in this work, we first evaluate satellite-based irradiance compared to ground-based irradiance data. Next, we investigate the accuracy of using the

satellite-based meteorological data in long-term performance analysis of three test modules in the absence of ground-based data. We use (1) ground-based and (2) satellite-based data separately as input irradiance. We calculate 60 PR time series and performance loss rates (PLR) for each irradiance data using different filtering methods and performance metrics. As a representative PLR value, we used the mean value (excluding outliers) of the various PLR values obtained as suggested by IEA PVPS Task 13.

Table 6 provides a definition of the ground-based and satellite-based meteorological monitoring systems that have been used in this work. Ground G_{POA} (20˚ tilt and -4˚ azimuth from South) was monitored every minute between December 2015 and May 2019 by well-calibrated (and maintained) thermopile pyranometer installed on the outdoor test site of SUPSI, in Canobbio (Switzerland, 46.02°N and 8.91°E). The temperature of the modules were monitored using a Pt100 sensor attached on the rear side of the modules at 1-minute intervals during the outdoor deployment. Satellite-derived G_{POA} (20˚ tilt and -4˚ azimuth from South) and ambient temperature (at 2 meters height) data were retrieved with 5-minute frequency for the same duration of time from Solargis (a company that provides satellite-derived weather data for solar investments and analysis) [41].

The Solargis satellite-based solar radiation is calculated by numerical models, which are parameterised by a set of inputs characterising the cloud transmittance, state of the atmosphere and terrain conditions. In the Solargis approach, the clear-sky irradiance is calculated by the simplified SOLIS model [42]. This model allows fast calculation of clear-sky irradiance from the set of input parameters. The clouds are the most influential factor, modulating clear-sky irradiance. The effect of clouds is calculated from the satellite data in the form of a cloud index (cloud transmittance). All-sky irradiance in each time step is calculated by coupling the clear-sky global horizontal irradiance with the cloud index. More information regarding the Solargis satellite-based data is presented in this report [43].

Table 6: Definition of ground-based and satellite-based input meteorological data.

	Ground-based Monitoring System	**Satellite-based Monitoring System**
G_{POA}	On-site pyranometer (properly maintained and calibrated)	Satellite-derived
Module Temperature	Temperature sensor (back of module) (properly maintained and calibrated)	Calculated from estimated ambient temperature using Ross' approximation [44]

We evaluated the satellite-based irradiance data with respect to ground-based data. The G_{POA} values below 50 W/m^2 and above 1250 W/m^2 were filtered out to exclude anomalies. The time-series of normalised bias of satellite-derived G_{POA} ($G_{POA,satellite}$) for monthly temporal resolution was calculated using the following formulas with respect to ground-based G_{POA} ($G_{POA,ground}$):

$$\text{Norm. Bias}_{G_{POA}}[\%] = \frac{G_{POA,satellite} - G_{POA,ground}}{G_{POA,ground}} \times 100$$

Figure 6 shows monthly normalised bias series of $G_{POA,satellite}$. The monthly $G_{POA,satellite}$ is overestimated in summers and underestimated in winters (sinusoidal-like trend). Rdtools' CSI clear sky filtering did not have significant impact on the accuracy of monthly $G_{POA,satellite}$. It is important to understand effect of this sinusoidal-like bias on PLR computation. More detailed information regarding uncertainties of satellite data and performance ratio (PR) (satellite vs ground irradiance data) can be found in section 3.1.5.

Table 7: Summary of the data filtering techniques used in this work. The parameters changed are written in bold.

Irradiance Threshold	**Clear Sky**
• **50** W/m^2 < G_{POA} < 1250 W/m^2 • **100** W/m^2 < G_{POA} < 1250 W/m^2 • **200** W/m^2 < G_{POA} < 1250 W/m^2 • **500** W/m^2 < G_{POA} < 1250 W/m^2	• RdTools' CSI [49]
Power Threshold	**Power - Irradiance** [50]
• 0.01 x P_{nom} < P_{meas} < **1.2** x P_{nom} • 0.01 x P_{nom} < P_{meas} < **1.02** x P_{nom}	• LQ: **20th**, UQ: **80th** • LQ: **10th**, UQ: **90th** • LQ: **5th**, UQ: **95th**
Instantaneous PR (5-minute)	
• **±1**σ • **±2**σ • **0.3** < PR_{ins} < **1.2**	
G_{POA}: Plane of array irradiance, P_{nom}: Nominal power, P_{meas}: measured power, PR_{ins}: instantaneous PR, LQ: Lower quantile, and UQ: Upper quantile.	

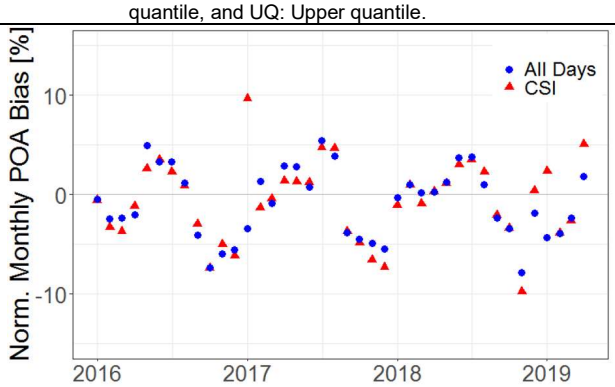

Figure 6: Time-series of normalised bias for monthly aggregated satellite-derived G_{POA} with respect to ground-measured insolation ("All days": no clear sky filter and "CSI": RdTools' clear sky filter).

In this work, various PLR analysis methods have been applied to each long-term performance of PV modules. Each PLR analysis method is a combination of data filtering method, performance metric and statistical analysis tool. We created 60 PLR analysis methods using 30 different data filtering methods, two different performance metrics and one statistical analysis tool. The data filtering methods were created using irradiance, power, instantaneous PR, power-irradiance relation and clear-sky filters with different thresholds (Table 7). We initially created 15 data filtering methods by combining four of the above-mentioned data filtering approaches (irradiance threshold, power threshold, power-irradiance and instantaneous PR filters). Then, each data filtering method was made with and without CSI clear sky filtered input data for G_{POA}. Hence, in total, 30 different filtering methods were created for the PLR analysis.

The monthly aggregated PR and temperature corrected PR (PR_{cor}) were used as the main performance metrics in the long-term performance analysis of the three PV modules installed at SUPSI [45]. PR is calculated from the ratio between the energy yield of an array (Y_f) and reference yield calculated over a given temporal interval (Y_r) [46]. A statistical method, the seasonal and trend decomposition using LOESS (STL), was used to compute PLR since it is insensitive to outliers and seasonality [47, 48].

Figure 7 shows a conceptual flowchart of our PLR analysis approach, including data filtering, performance metrics and statistical method. Initially, long-term PV performance data was merged with satellite-based monitoring data. Then, 30 different data filtering methods were applied, and 30 time-series were created. For each time-series, monthly aggregated PR and PR_{cor} metrics were calculated. This results in 60 monthly performance metric time-series in total (30 for PR and 30 for PR_{cor} series). Then, the STL statistical method was applied on PR and PR_{cor} time-series to compute PLR. Therefore, 60 PLR using satellite-based monitoring ($PLR_{satellite}$) were calculated for each PV performance data. The same approach was applied using ground-based meteorological data as well. Hence, 60 PLR using ground-based monitoring (PLR_{ground}) were created for each PV performance data in addition to 60 $PLR_{satellite}$.

For each PV module, 60 $PLR_{satellite}$ and 60 PLR_{ground} values were computed by following the methods summarised in Figure 7. Figure 8a shows the 60 PLR_{ground} values of one of the monitored modules (module-3). The PLR_{ground} values are mostly similar, but we observe some outliers. PLR_{ground} values outside a band of ±2σ (standard deviation) were excluded to determine $PLR_{ref,ground}$ which is the mean of the remaining PLR_{ground} values (Figure 8a). Using the mean of the different PLR_{ground} values as a reference ($PLR_{ref,ground}$) is an approach proposed in the work of IEA PVPS Task 13 [51].

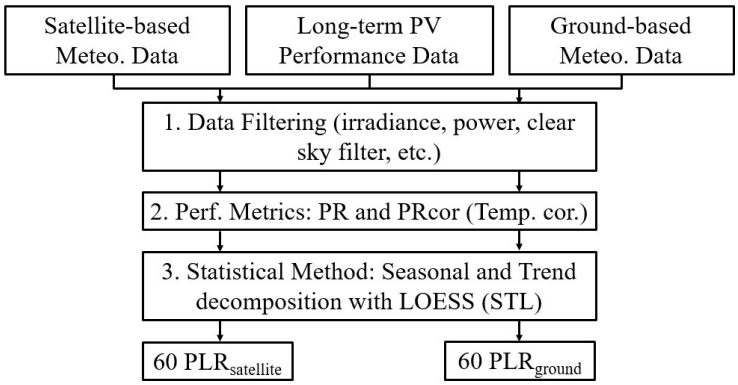

Figure 7: Conceptual flowchart of our PLR analysis approach including data filtering, performance metric computation and statistical method steps.

Figure 8b shows the 60 $PLR_{satellite}$ values with the $PLR_{ref,ground}$ for the same module, module-3. The $PLR_{satellite}$ values are more scattered than the PLR_{ground} values, which may be due to uncertainty of satellite data and temperature modelling. The process was repeated for the other two modules as well (not shown). The method explained previously to determine the $PLR_{ref,ground}$ using PLR_{ground} values was utilised to determine a single representative $PLR_{satellite}$ ($PLR_{ref,satellite}$) from the computed $PLR_{satellite}$ values using various data filtering methods and performance metrics. The $PLR_{satellite}$ values outside a band of ±2σ were removed and the mean of the remaining $PLR_{satellite}$ values represents the $PLR_{ref,satellite}$.

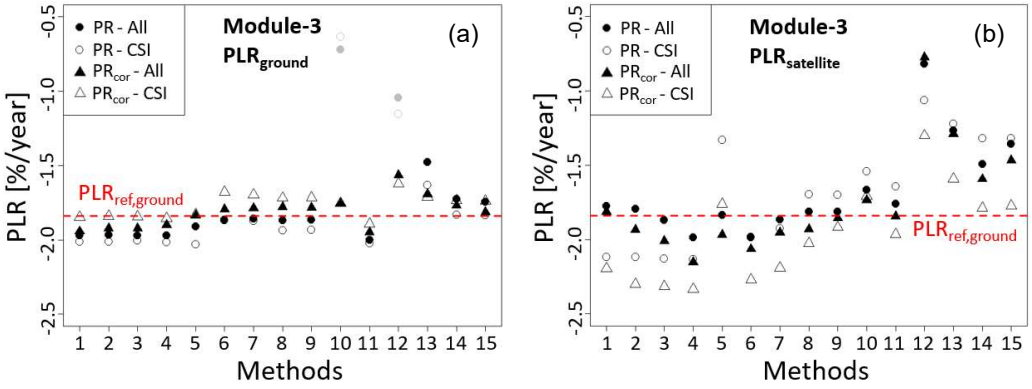

Figure 8: (a) PLR_{ground} values with $PLR_{ref,ground}$ (red dashed line), the mean of the remaining (without outliers) PLR_{ground} values (dark) for module-3. Gray PLR_{ground} values are outliers. (b) 60 $PLR_{satellite}$ values with $PLR_{ref,ground}$ for module-3.

Figure 9 shows the $PLR_{ref,ground}$ and $PLR_{ref,satellite}$ of each module. For module-3, the $PLR_{ref,ground}$ and $PLR_{ref,satellite}$ are almost identical whereas for module-1 and module-2, $PLR_{ref,satellite}$ values fall slightly outside of the 1σ band surrounding $PLR_{ref,ground}$. However, there are overlaps between the standard deviations computed for $PLR_{ref,ground}$ and $PLR_{ref,satellite}$ for the both modules. Considering the relatively large uncertainty associated to outdoor measurements, satellite-derived insolation data and long-term performance analysis, we do not spot major differences between the $PLR_{ref,ground}$ and $PLR_{ref,satellite}$ calculated for each module. This demonstrates that an accurate long-term performance assessment using satellite-based monitored data instead of ground-based monitored data is in principle possible by computing the mean of various PLR values obtained from different data filtering methods and performance metrics. Averaging computed PLRs suggested by IEA Task 13, will be used to compute PLR of the modules mentioned in the subsection 3.1.2. More details on this work can be found in [40].

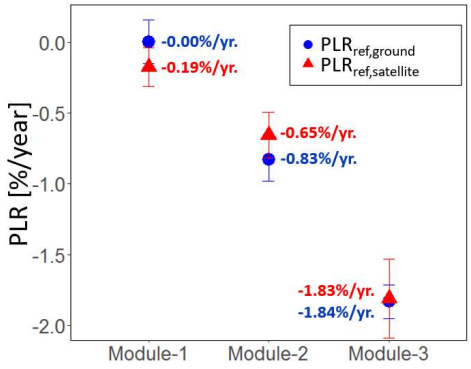

Figure 9: Reference performance loss rates using ground- and satellite-based monitoring, $PLR_{ref,ground}$ and $PLR_{ref,satellite}$, of the three modules with their standard deviation.

3.1.5 Uncertainty of Performance Ratio using Ground-based vs Satellite-derived Meteorological Data

PV systems' short- and long-term performances (PLR) are often evaluated by analysing performance ratio (PR) computed using satellite-derived insolation data sets which are associated with higher uncertainties. In order to evaluate the performance of a PV system accurately, the uncertainty contribution needs to be carefully computed. For this reason, we quantified: (1) the accuracy of two satellite-derived insolation data-set (CAMS and Solargis) with respect to the irradiance ground measurement obtained by properly maintained sensors; and (2) their effect on the uncertainty of PR computed using satellite-derived insolation with different temporal resolutions.

Figure 10 shows that since the uncertainty of satellite-derived insolation decreases with longer temporal intervals, the PR uncertainty also decreases. The uncertainties of weekly, monthly and yearly PR computed using Solargis data are only 1.5%, 0.9% and 0.2% higher than the reference case, 4.7%, the uncertainty of PR estimated using measured data by well-maintained pyranometer, respectively. Depending on the purpose of use, different time resolutions and satellite-derived data quality can be preferred for analysis using PR as a performance index. If only weekly, monthly or annual PR is the matter to check the general status of a PV system, PR values, which have an uncertainty of less than 8%, can be obtained using CAMS and Solargis satellite-derived insolation data without having to deal with regular calibration and maintenance of an on-site radiation sensor. However, there is a trade-off as accuracy and precision drop while cost and time savings are achieved. In addition, it should be reminded that in this analysis, ground-based PR uncertainty was estimated using the uncertainty of ground-based GPOA measured with a well-maintained and recalibrated secondary class pyranometer. However, depending on various conditions, the uncertainty of ground-based irradiance measurement could be up to 8%, as mentioned previously [52]. This could result in PR uncertainty greater than 4.7%.

In addition, to analyse a PV system's long-term performance, changes in PR over time are usually computed using different statistical tools (e.g., linear regression (LR), seasonal-trend decomposition using LOESS (STL), year-over-year (YoY), etc. [48]). The amount of data points is a factor which affects the confidence intervals (usually with 95% confidence) of the final result, called performance loss rate (PLR) or degradation rate (DR). If there are more data points and a regression model is used (e.g., LR, STL, etc.), the range of confidence intervals of PLR is expected to be smaller, which means PLR is more accurate and precise. However, more data points mean smaller time intervals, such as daily PR, and daily PR has larger uncertainty than yearly PR. There is a trade-off between PR uncertainty (lower uncertainty and fewer data points for longer temporal intervals) and the number of data points (higher uncertainty and more data points for shorter temporal intervals) for accurate and precise long-term performance analysis. This trade-off will be further investigated.

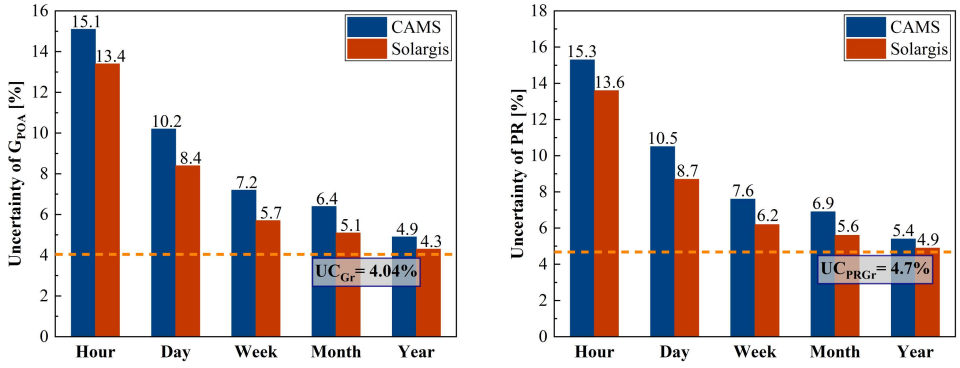

Figure 10: Uncertainties (k=2) of (left) satellite-derived CAMS and Solargis G_{POA} and (right) PRs computed using ground-based and satellite-derived CAMS and Solargis G_{POA}. Pyranometer uncertainty is 2.7% (k=2) at 1000 W/m^2.

3.2 Work Package 2: Outdoor Realistic Worst Case Conditions in the Building Environment

This work package aims to accurately monitor BIPV modules parameters in realistic and worst-case conditions, building different setups for façade and sloped roof mounting in SUPSI outdoor facilities. Task 1, which is procurement and initial characterisation of the modules, is represented in Section 3.2.1. The outdoor mock-ups are presented in Section 3.2.2 (Task 2). Task 3 and 4 are on-going since they are monitoring of the outdoor test mock-ups, and we need minimum 1 year of data to conclude these tasks.

3.2.1 Procurement and Characterisation of the Modules

The modules in this project are presented in Table 8 together with their use (outdoor mock-up, indoor tests and reference). The first four module technologies are procured for this project. We already had the last three module technologies, and we were monitoring their long-term performance in BIPV configurations previously at SUPSI Trevano campus. In this project, we continue to monitor their long-term performance. There are two modules with laminated temperature sensor (behind a cell) (fourth module technology in Table 8, PERC – BIPV-façade). They have been installed on the outdoor mock-up together with two modules with the same technology (without laminated sensor). In this way, the temperature difference between cell and module can be monitored, and we can be sure that there is no additional degradation mechanism due to laminated sensor by comparing modules with and without laminated sensor.

Table 8: Number of the modules in this project together with their use.

	Module Technology	Outdoor Mock-ups	Indoor Accelerated Tests (TC + HS)	Reference (Dark room)
1	**Halfcut PERC**	4	5	1
2	**Interdigitated back contacted (IBC)**	4	5	1
3	**Halfcut Heterojunction (HJT)**	4	5	1
4	**PERC – BIPV-façade**	4	4	1(+2)
5	**PERC – BIPV-roof (4+ years aged)**	2	2	1(+1)
6	**Al-BSF (G/EVA/BS) (4+ years aged)**	2	-	-
7	**Al-BSF (G/PVB/G) (4+ years aged)**	2	-	-

All the procured modules have been tested by performing visual inspection (VI), electroluminescence (EL), maximum power measurement (Pm), wet leakage test (WL), insulation test, temperature coefficient measurement (TCO) and performance at different irradiance levels (GCO). All the modules for the outdoor mock-ups have been installed. The measurement above will be performed again after indoor accelerated tests and outdoor monitoring.

3.2.2 Design and Building of BIPV Mock-ups

The procured modules were installed in different configurations on the outdoor testing area of the SUPSI Mendrisio campus in the South of Switzerland. This task aims to perform accurate and high-quality monitoring of BIPV modules' performance parameters in realistic and worst-case conditions. The duration of a research project (3-4 years) is generally not long enough to detect the performance degradation of PV modules (if the modules are well manufactured). Therefore, besides BIPV configuration, modules were installed to an outdoor test stand with additional stresses in order to trigger and accelerate degradation and failure modes. However, those stresses must be field representative and should not cause any degradation mechanisms that are not seen in the field. The analyses under Work Package 1 defined the most critical and common additional stresses of BIPV configurations. Those stresses are used to accelerate the degradation of the modules. The additional accelerated stresses are as follow:

1. **Heat blanket at the rear side of the modules (**Figure 11**):** The aim is to increase operating module temperature and reach above 70˚C around four hours of each day to accelerate ageing. In this way, 175.2 hours of operation at above 70˚C (minimum T_{98} limit in IEC TS 63126) can be reached in a few months instead of a year.

2. **Artificial shadow stress by using shadow mask:** The aim is to create more realistic BIPV operating condition. The effect of shadow stress on the performance and reliability of modules, module materials, and by-pass diode are monitored by using shadow mask.

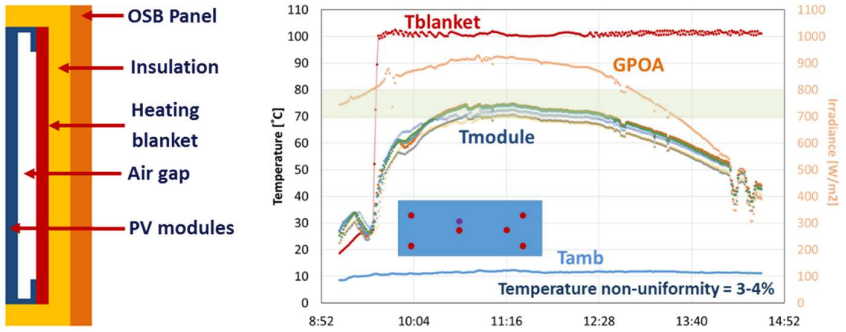

Figure 11: (Left) Simple drawing of heat blanket design and (Right) temperature profiles from experimental measurements.

Table 9 shows the modules and their installation configurations. Modules are grouped for different experiments since it is impossible to compare all of them simultaneously due to too wide spread of parameters.

The **first experiment** is the continuation of the Test Stand-1. The modules were installed in BIPV-insulated configuration, and one module from each type have a heat blanket at backside to accelerate ageing due to high operating temperature. The aim is to accelerate ageing of the modules that were open-rack installed before and to mimic degradation mechanisms of the insulated modules that have been observed previously (i.e., cell crack, interconnect damage and finger failure).

The PERC modules in BIPV-ventilated configuration in the Test Stand-2 are used to continue the outdoor deployment of them in the **second experiment**. Two modules were installed in BIPV-ventilated configuration, and one of them have a shadow mask to accelerate degradation due to shadow stress.

In the **third experiment**, a set of three different procured PV modules (Halfcut PERC, halfcut HJT and IBC) became part of the outdoor test stands for monitoring of BIPV conditions and worst-case conditions. The modules operate in four conditions; open-rack, BIPV-insulated, BIPV-insulated with heat blankets and BIPV-insulated with a shadow mask. By comparing performance of the modules in open-rack and BIPV insulated configurations, effect of additional stresses due to BIPV operating condition can be evaluated. In parallel, indoor qualification and reliability tests are performed that will add more quantitative data to outdoor results.

In the **fourth experiment**, the BIPV modules, which were installed on the 'Pregassona' building in Lugano became part of the outdoor experiments. The modules were installed as rain screen façade. Two of the modules have no shadow stress, while the other two modules have a shadow mask to accelerate degradation. Moreover, in each configuration (with and without shadow mask configurations), there is a module with an integrated temperature sensor to monitor cell temperature. These modules' indoor qualification/reliability tests (hot-spot endurance) have already started.

Table 9: Module types and their installation configurations for outdoor deployment.

Experiment Number	Module Type	Installation Configuration
1	- G/EVA/BS (from Test Stand-1) - G/PVB/G (from Test Stand-1)	- BIPV-Insulated (Roof) - BIPV-Insulated (Roof) with heat blankets
2	- G/EVA/BS	- BIPV-Ventilated (Roof)

	(PERC module from Test Stand-2)	- BIPV-Ventilated (Roof) with shadow mask
3	- Interdigitated Back Contacted (IBC) - Half-cut Hetero Junction Technology (HJT) - Half-cut PERC	- Open rack - BIPV-Insulated (Roof) - BIPV-Insulated (Roof) with heat blankets - BIPV-Insulated (Roof) with shadow mask
4	- G/EVA/G PERC coloured module (Custom BIPV product)	- BIPV-Ventilated (Façade) - BIPV-Ventilated (Façade) with shadow mask

As shown in Figure 12, the outdoor mock-ups were installed, and the monitoring started at the end of May 2022. We are monitoring GHI, DHI and GPOA (30° and 90° tilts), module temperature, cell temperature of 2 modules, ambient temperature, hot spot and junction box temperatures (only for modules with shadow mask) with 1-minute intervals. In addition, all IV parameters together with IV curves are monitored every minute (Figure 13).

Figure 12: The REBIPV outdoor mock-ups.

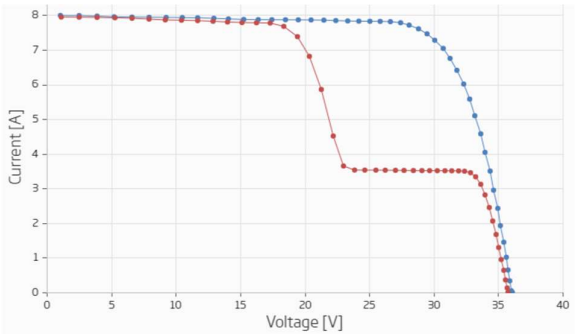

Figure 13: An example from the dashboard of monitored data which shows IV curves of two modules and one of them has shadow mask.

Figure 14 shows a module's thermography image and temperature profiles (not on the same day). As can be seen, by using the shadow masks, we create heat dissipation on both cell and diode parts of a module. Since we have temperature sensors behind the hot spot area and inside the junction box, we can monitor the temperature. The shadow mask is not a worst-case shadow but the hotspot temperature reaches 140°C and junction box temperature reaches about 90°C. As can be seen on Figure 15, depending on cell technology (breakdown voltage) and number of cells connected to a diode, temperature of hot spot varies. These are only preliminary results and more detailed analysis will be done.

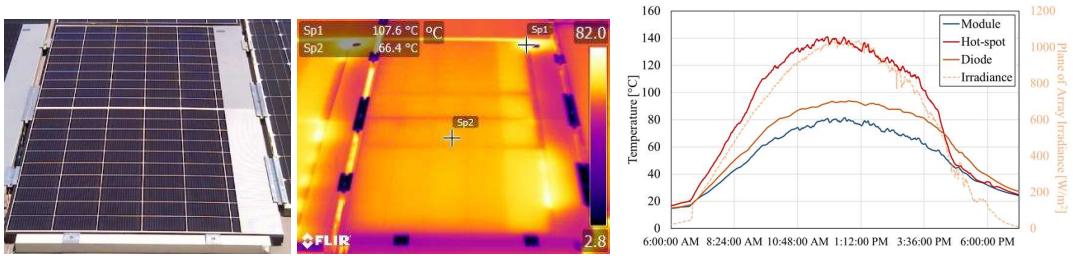

Figure 14: Thermography image and temperature profiles of a module with shadow mask.

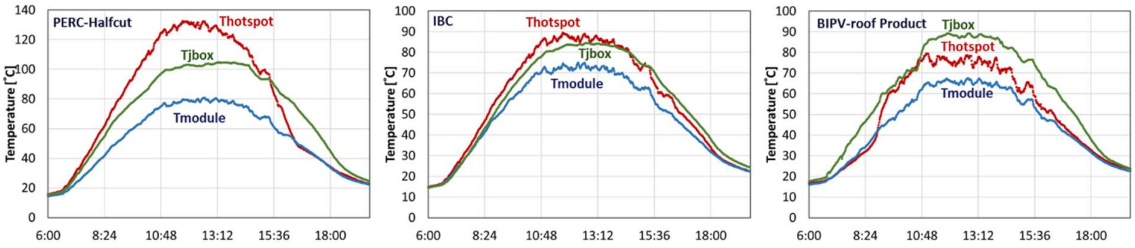

Figure 15: Temperature profiles of PERC, IBC and BIPV-rood product modules with shadow mask.

Figure 16 shows the temperature profiles of a module type in open-rack, BIPV-Insulated and heat blanket configurations. The temperature of the BIPV-insulated module reaches 80°C and the maximum temperature difference between open-rack and BIPV-insulated modules is about 25°C. The BIPV-insulated module spent around 4 hours above 70°C. The module with heat blanket spent 6.5 hours above 70°C. The stand will be improved after measuring these modules' performance in our laboratory in January 2023. After the improvement, more hours will be spent above 70°C. Until now this module spent almost 350 hours (2 times of 175 hours) above 70°C in 3.5 months. More detailed analysis will be done later.

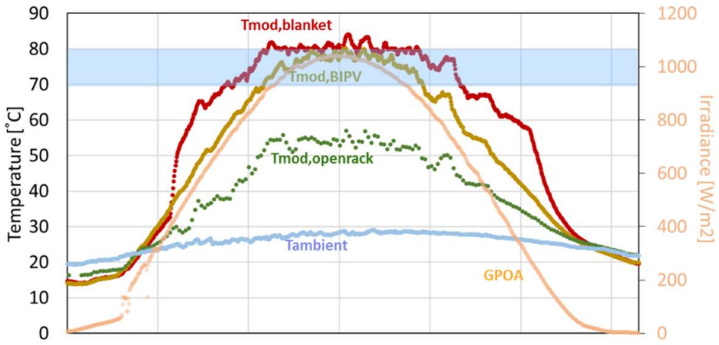

Figure 16: Temperature profiles of a module technology in open-rack, BIPV-insulated and heat blanket configurations.

3.3 Work Package 3: Accelerated Testing of BIPV Modules

This section is about accelerated testing in indoor (Task 1) and outdoor (Task 2). The outdoor accelerated tests using heat blanket and shadow masks are already mentioned in subsection 3.2.2. Subsection 3.3.1 describes the current situation regarding the indoor accelerated tests.

3.3.1 Indoor accelerated tests

Based on the analysis results in Work Package 1, it was decided to conduct thermal cycle (TC) and hot spot endurance (HS) tests. Both tests are done in standard testing conditions according to IEC 61215:2021, and harsher testing conditions according to IEC TS 63126:2020. Table 10 shows the use of modules along with the tests (indoor and outdoor) to be performed and the number of modules for each test/mock-up. From this table, the relationship between indoor tests and outdoor models can be seen more clearly. The modules, which were installed in BIPV-insulated with shadow mask configuration, will be tested for hot-spot endurance. Also, the modules, which were installed in BIPV configuration and installed with a heating blanket, will be performed thermal cycling test. There is no planned indoor accelerated test for the last two module technologies in Table 10 because there is no extra module.

As shown in Table 10, two thermal cycling (TC) tests are planned to be performed. First 200 cycles of the standard TC (IEC 61215-2:2021) finished with four modules (also an additional PERC shingled module). After 200 cycles, electrical characterisation of the modules (Pm, EL, VI, WL and insulation tests) were performed. Then, TC continued until 600 cycles in total, and after each 100 cycles, the same electrical characterisation methods were performed. The second TC test (100 + 100 cycles) will be done using the same type of modules but this time the maximum temperature of TC will be 95˚C instead of 85˚C as suggested in IEC TS 63126 for modules operating at elevated temperatures.

Preliminary analysis of the first TC test is shown in Figure 17. For now, modules are anonymised. Clearly, Module-3 and -4 lost some performance due to loss in FF. For Module-3, it seems there is humidity penetration, which is visible around the cell edges, and finger detachment, which explains increase series resistance and loss in FF. For module-4, there are damaged cell connections, which caused loss in FF. There are also hot areas which causes permanent hot spots. More detailed analysis will be done after performing the second TC test.

Table 10: The use of modules, the tests to be performed (indoor and outdoor) and the number of modules for each indoor test and mock-up. The numbers in bold means that test is finished. If it is outdoor test, it means monitoring started. The numbers in Italic means that test hasn't started yet.

Module Technology		Planned Indoor Accelerated Tests (IEC61215:2021)					Outdoor Mock-up Configurations			
		Thermal Cycling (MQT11)		Hot-spot endurance (MQT09)						
		Standard (-40 - +85C, 600 cyc.)	New (-40 - +95C, 200 cyc.)	Standard (50C,1h/5h)	New-1 (60C,1h/5h)	New-2 (70C,1h/5h)	Open -rack	BIPV -Ins.	BIPV-Ins. & Shadow mask	Heat blanket
1	Halfcut PERC	**1**	*1*	*1*	*1*	*1*	**1**	**1**	**1**	**1**
2	IBC	**1**	*1*	*1*	*1*	*1*	**1**	**1**	**1**	**1**
3	Halfcut HJT	**1**	*1*	*1*	*1*	*1*	**1**	**1**	**1**	**1**
4	PERC – BIPV-façade	-	*1*	*1*	-	*1*	-	**1**	**1**	-
5	PERC – BIPV-roof (4+ years aged)	-	-	*1*	-	*1*	-	**1**	**1**	-
6	Al-BSF (G/EVA/BS) (4+ years aged)	-	-	-	-	-	-	**1**		**1**
7	Al-BSF (G/PVB/G) (4+ years aged)	-	-	-	-	-	-	**1**		**1**

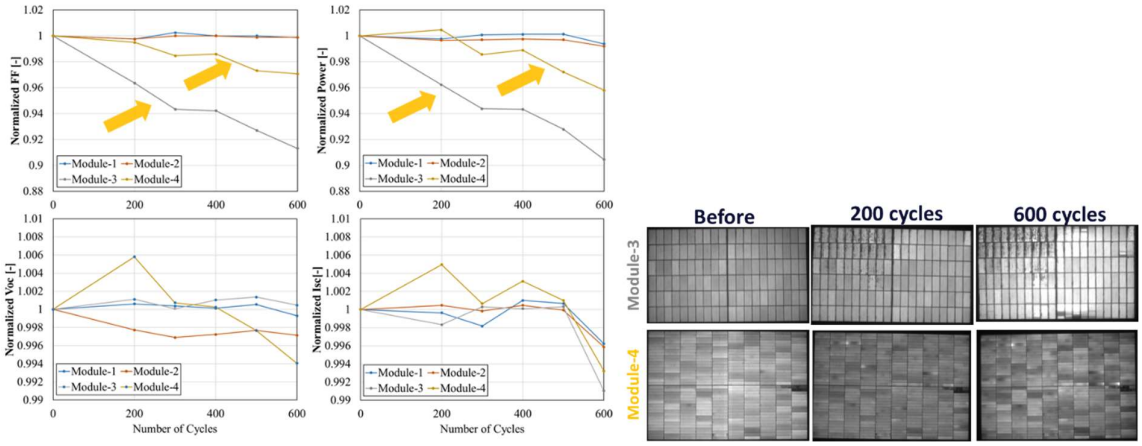

Figure 17: (Left) Normalised IV values and (Right) EL images at initial, intermediate and final steps for the Thermal Cycling test (-40C - +85C, 600 cycles) (only Module-3 and -4).

There are two expected outcomes from these TC tests. First, long-term performance of the modules installed in the outdoor mock-ups (especially modules in BIPV-insulated and heat blanket configurations) will be compared with indoor TC tests in standard and extended conditions (i.e., extended number of cycles and higher maximum temperature). Secondly, it has been shown that in a hot climate zone, e.g., Chennai India, ~630 cycles (−40˚C to +85˚C) is necessary to accumulate a same amount of damage as 25 years of lifetime of a PV module [35]. Moreover, to detect manufacturing solder failures, more than 200 cycles could be needed [53]. Therefore, there are interest on TC with extended number of cycles. In addition, it has been shown by modeling that by increasing the maximum temperature to 95˚C, the same amount of stress can be generated at 200 cycles as in 600 cycles of TC (-40˚C to +85˚C) [35]. Hence, it will be interesting to compare results from TC at standard temperature range but extended number of cycles (-40 to +85˚C, 600 cycles) and TC at larger temperature ranges but 200 cycles (-40 to +95˚C, 200 cycles).

Additionally, hot-spot endurance (HS) tests in standard conditions (IEC 61215-2:2021) are also started. Module technology 4 and 5 in Table 10 were tested according to the IEC 61215-2, and no problem was observed (Figure 18). The test duration will be extended until there is a failure to understand the durability of the modules. In addition, HS test at a higher testing temperature will be performed, as shown in Table 10. The results from outdoor mock-ups will be compared with indoor HS tests.

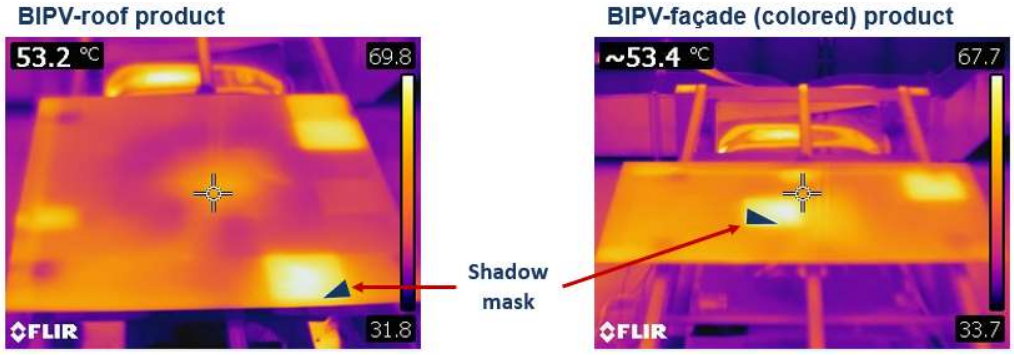

Figure 18: Thermography images of the modules during hot-spot endurance test according to IEC 61215-2.

4 Conclusion

We show that operating conditions and performance changes of the modules in open-rack and typical BIPV installation configurations (BIPV-ventilated for reduced rear-side ventilation and BIPV-insulated for restricted rear-side ventilation). The maximum operating temperature of the insulated BIPV modules reached slightly above 90°C in Southern Switzerland. These modules have around 23°C–27°C larger T_{98} compared with the same modules in open-rack because of restricted rear-side air ventilation. Similarly, the ventilated BIPV modules operated at higher temperatures than the open-rack modules (21°C higher T_{98}). Furthermore, all BIPV modules, including the façade module, were exposed to greater diurnal (day–night) temperature variations with respect to the open-rack modules. In the worst-case situation, the insulated modules on a tilted surface experienced more than 75°C temperature change, whereas the open-rack modules never experienced temperature changes greater than 50°C between day and night. The BIPV modules on a sloped roof surface were, therefore, exposed to larger thermal and thermo-mechanical stresses than the modules in a conventional open-rack configuration. These stresses could presumably accelerate the degradation of the polymeric materials in the module sandwich and cause damage to cells and metallic contacts. This could later cause higher degradation rates and shorten the lifetime of BIPV modules which calls for further investigation. According to IEC TS 63126, two insulated Al-BSF and the ventilated HJT BIPV modules ($70°C < T_{98} \leq 80°C$) operated at temperatures above the typical temperature ranges used in the qualification and safety tests of IEC 61215 and IEC 61730.

Moreover, we analysed the change in the modules' performance by performing PLR analysis using the monitored data during the outdoor exposure and STC power measurements at indoor before and after the outdoor exposure. First, we showed that since larger thermal stress accelerates UV-induced degradation of EVA, there could be loss in I_{sc} in BIPV configurations. In addition, due to larger thermo-mechanical stress, there could be damaged cells and metallization that cause FF loss (Test Stand-1). In addition, PV modules may have issues originated from their production, e.g., encapsulant material susceptible to UV and thermal stresses. In this case, the results from Test Stand-2 (c-Si, G/G, BIPV-ventilated prototype module) show that those issues could not be important for the safety and performance of conventional PV; however, for BIPV applications, imperfect production could be more significant since the operating conditions are more challenging than conventional PV.

Most importantly, modules operating in a BIPV configuration do not have to degrade faster. There could be faster degradation only if there are larger thermal and-or thermo-mechanical stresses. As shown from Test Stand-2 (c-Si, G/BS), if a ventilation chamber of a BIPV-ventilated module is well-designed, there will not be high enough thermal and thermo-mechanical stresses to cause BIPV-related accelerated degradation mechanisms. Last of all, the BIPV-ventilated façade module did not degrade after 2 years. However, it needs to be monitored for longer durations to be able to see possible effects of larger thermo-mechanical stress.

As explained in the Introduction section, this project is still on-going, and the next steps regarding different subjects are shown in the following subsections.

4.1 BIPV Module and System Analyses

As mentioned previously, due to delays and compensate unavailability of project data, Deliverable 1.4 (Evaluation of Long-term Performance Analysis Methods and Satellite-derived Insolation data for the long-term analysis, and long-term Performance Analysis of historic/existing data) is added to the project. In these analyses, long-term performance analysis of existing BIPV systems (i.e., 55 BIPV-roof systems in Switzerland [54]) and various other studies on the precision of performance ratio and long-

term performance analysis have been conducted. The methods used in these analyses will be used to analyse the data from the installed test stands within this or other projects. There are few studies still ongoing, for example, detailed long-term performance analysis of existing BIPV test stands (SUPSI's historical data) and uncertainty analysis of performance ratio (PR) and performance loss rate (PLR) using ground and satellite-derived insolation data. These studies will be finalised, and manuscripts will be written.

As mentioned in subsection 3.1.2, we performed non-destructive characterisation of modules operated in BIPV configurations. Currently, we are analysing all the data we have for these modules and finding correlations between different analysis methods (outdoor data, indoor electrical characterisation and non-destructive material characterisation). There are interesting results, and a manuscript will be written in early 2022 to be published.

4.2 Outdoor Mock-ups

The current situation regarding the outdoor test mock-ups is already mentioned in subsection 3.2.2. The monitored data will be properly analysed after there is enough amount of data depending on type of analysis.

4.3 Accelerated Ageing Tests

Table 10 shows the planned accelerated ageing tests. As mentioned previously, we have started to perform the accelerated ageing tests. The plan is to finish TC test beginning of 2023 in worst-case. The HS tests will take more time but they need to be finished before April-2023. Moreover, there will be intermediate measurements (Pm, EL, VI, WL and insulation), which will take some time.

5 National and international cooperation

- Collaboration with École polytechnique fédérale de Lausanne (EPFL) in Swiss National Science Foundation (SNF) project (IZCOZ0_182967/1).
- Material characterisation of the long-term outdoor aged BIPV modules is carrying out together with OFI - Österreichisches Forschungs- und Prüfinstitut under Cost Action PEARL PV (https://www.pearlpv-cost.eu/).
- Collaboration with Dr. Abdulkerim Gok through Cost Action PEARL PV (https://www.pearlpv-cost.eu/) on long-term performance analyses of BIPV modules, which started before the start of this project. Published work [55, 36].

6 Publications

- E. Özkalay, G. Friesen, M. Caccivio, P. Bonomo, A. Fairbrother, C. Ballif and A. Virtuani, *"Operating Temperatures and Diurnal Temperature Variations of Modules Installed in Open-Rack and Typical BIPV Configurations,"* IEEE Jour. of PV, 2022
- A. Fairbrother, H. Quest, E. Özkalay, P. Wälchli, G. Friesen, C. Ballif and A. Virtuani, *"Long-Term Performance and Shade Detection in Building Integrated Photovoltaic Systems,"* Solar RRL, 2022.

- E. Özkalay, G. Friesen, A. Virtuani, A. Fairbrother, M. Caccivio, C. Ballif, "*Long-term Performance Analysis of PV Modules Installed in Open-rack and BIPV Mounting Configurations*", Oral presentation at 8th WCPEC, Milano, 2022.
- E. Özkalay, A. Virtuani, A. Fairbrother, A. Skoczek, G. Friesen, C. Ballif, "*How does the use of satellite-derived insolation data impact the accuracy of Performance Ratio estimates?*", Poster presentation at 8th WCPEC, Milano, 2022.
- E. Özkalay, A. Virtuani, A. Fairbrother, A. Skoczek, G. Friesen, M. Caccivio, C. Ballif, "*Quantifying Performance Loss Rates of Photovoltaic Modules using Ground-based vs Satellite-based Meteorological Data*", Poster presentation at PVTagung, 2022.
- M. Caccivio, E. Özkalay, D. Chianese, "*Photovoltaïque intégré au bâti et ombrage*", bulletin.ch, 2022.
- E. Özkalay, G. Friesen, A. Fairbrother, C. Ballif and A. Virtuani, "*Monitoring the Operating Temperatures of Modules in Open-Rack and Typical BIPV Configurations*", Conference Proceedings of IEEE PVSEC (Oral), 2021.
- E. Özkalay, A. Virtuani, A. Fairbrother, A. Skoczek, G. Friesen, and C. Ballif, "*Quantifying Performance Loss Rates of Photovoltaic Modules Using Ground-based and Satellite-based Meteorological Data*", Conference Proceedings of EUPVSEC (Oral), 2021.
- E. Özkalay, G. Friesen, A. Fairbrother, C. Ballif and A. Virtuani, "Operating Temperatures of Modules in Open-Rack and BIPV Configurations", 2021, Poster presentation at PVTagung, 2021.
- A. Gok, E. Ozkalay, G. Friesen and F. Frontini, "Power loss modes of building-integrated photovoltaic modules: An analytical approach using outdoor I-V curves," *IEEE Journal of Photovoltaics,* 2021.
- A. Gok, E. Ozkalay, G. Friesen and F. Frontini, "The influence of operating temperature on the performance of BIPV modules," *IEEE Journal of Photovoltaics,* 2020.

References

[1] J. F. Weaver, "Humans have installed 1 terawatt of solar capacity, generated over 1 petawatt of solar electricity in 2021," *PV Magazine USA,* 14 March 2022.

[2] IEA, "Snapshot of Global PV Market 2021," International Energy Agency, 2021.

[3] IRENA, "Renewable Power Generation Costs in 2020," International Renewable Energy Agency, 2021.

[4] IRENA, "Global energy transformation: A roadmap to 2050 (2019 edition)," International Renewable Energy Agency, Abu Dhabi, 2019.

[5] IRENA, "Renewable power generation costs in 2018," International Renewable Energy Agency, Abu Dhabi, 2019.

[6] BfE, "Energiestrategie 2050 Monitoring-Bericht 2020," 2020.

[7] BfE, "Bundesamt für Energie," 2019. [Online]. Available: https://www.bfe.admin.ch/bfe/de/home/news-und-medien/medienmitteilungen/mm-test.msg-id-74641.html. [Accessed 2020].

[8] BIPVBOOST, "Update on BIPV market and stakeholder analysis," 2019.

[9] T. Zhang, M. Wang and H. Yang, "A Review of the Energy Performance and Life-Cycle Assessment of Building-Integrated Photovoltaic (BIPV) Systems," *Energies,* vol. 11, no. 11, p. 3157, 2018.

[10] M. Perez and V. Fthenakis, "A lifecycle assessment of façade BIPV in New York," *37th IEEE Photovoltaic Specialists Conference,* pp. 3271-3276, 2011.

[11] K. Menoufi, D. Chemisana and J. I. Rosell, "Life Cycle Assessment of a Building Integrated Concentrated Photovoltaic scheme," *Applied Energy,* vol. 111, pp. 505-514, 2013.

[12] IEA, "Renewables 2019: Market analysis and forecast from 2019 to 2024," International Energy Agency, Paris, 2019.

[13] E. Saretta, P. Bonomo and F. Frontini, "Active BIPV Glass Facades: Current Trends of Innovation," in *Glass Performance Days*, 2017.

[14] T. James, A. Goodrich, M. Woodhouse, R. Margolis and S. Ong, “Building-Integrated Photovoltaics (BIPV) in the Residential Sector: An Analysis of Installed Rooftop System Prices,” NREL, 2011.

[15] PVsites, “BIPV market and stakeholder analysis and needs,” 2016.

[16] n-tech Research, “BIPV technologies and markets: 2015 - 2022,” 2015.

[17] Solararchitecture. [Online]. Available: https://solarchitecture.ch/solaris-416/. [Accessed 2020].

[18] F. Frontini, S. M. Bouziri, G. Corbellini and V. Medici, “S.M.O solution: an innovative design approach to optimize the output of BIPV systems located in dense urban environments Francesco,” *Energy Procedia 91,* vol. 91, pp. 945-953, 2016.

[19] P. Heinstein, C. Ballif and L. E. Perret-Aebi, “Building Integrated Photovoltaics (BIPV): Review, Potentials, Barriers and Myths,” *De Gruyter,* vol. 3, no. 2, pp. 125-156, 2013.

[20] T. Nordmann and L. Clavadetscher, “Understanding temperature effects on PV system performance,” in *World Conference onPhotovoltaic Energy Conversion*, 2013.

[21] A. Virtuani and T. Sample, “Modification to the Standard Reference Environment (SRE) for Nominal Operating Cell Temperature (NOCT) to Account for Building Integration,” in *24th EU PVSEC*, Hamburg, 2009.

[22] H. Hu, W. Gambogi, K. R. Choudhury, L. Garreau-Iles, T. Felder, S. MacMaster, O. Fu and T.-J. Trout, “Field analysis and degradation of modules and components in distributed PV applications,” in *35th European Photovoltaic Solar Energy Conference and Exhibition*.

[23] D. Jordan, T. Silverman, J. Wohlgemuth, S. Kurtz and K. VanSant, “Photovoltaic failure and degradation modes Dirk,” *Progress in Photovoltaics: Research and Applications,* vol. 25, p. 318–326, 2017.

[24] P. Bonomo, I. Zanetti, F. Frontini, M. Donker, F. Vossen and W. Folkerts, “BIPV Products Overview for Solar Building Skin,” in *EUPVSEC*, 2017.

[25] SUPSI and SEAC, “Building Integrated Photovoltaics: Product overview for solar building skins Status Report 2017,” 2017.

[26] IEC, “IEC TS 63126:2020 ED1 Guidelines for qualifying PV modules, components and materials for operation at high temperatures,” International Electrotechnical Commission, 2020.

[27] IEC, “IEC 61215-2:2016 Terrestrial photovoltaic (PV) modules - Design qualification and type approval - Part 2: Test procedures,” International Electrotechnical Commission, 2016.

[28] IEC, “IEC 61730-2:2016 Photovoltaic (PV) module safety qualification - Part 2: Requirements for testing,” International Electrotechnical Commission, 2016.

[29] A. Fairbrother, A. Virtuani and C. Ballif, “Outdoor operating temperature of modules in BIPV and BAPV topologies,” in *37th European Photovoltaic Solar Energy Conference and Exhibition*, 2020.

[30] M. Koehl, S. Hamperl and M. Heck, “Effect of thermal insulation of the back side of PV modules on the module temperature,” *Progress in Photovoltaics: Research and Applications,* vol. 24, no. 9, pp. 1194-1199, 2016.

[31] Z. C. Holma, A. Descoeudres, L. Barraud, F. Z. Fernandez, J. P. Seif, S. De Wolf and C. Ballif, “Current losses at the front of silicon heterojunction solar cells,” *IEEE Journal of Photovoltaics,* pp. 7-15, 2012.

[32] D. Jordan, S. Kurtz, K. VanSant and J. Newmiller, “Compendium of photovoltaic degradation rates,” *Progress in Photovoltaics: Research and Applications,* no. 24, p. 978–989, 2016.

[33] H. Hu, W. Gambogi, K. Choudhury, L. Garreau-Iles, T. Felder, S. Macmaster, O. Fu and T. Trout, “Field analysis and degradation of modules and components in distributed PV applications,” in *35st EUPVSEC*, 2018.

[34] D. Rajiv, S. Chattopadhyay, V. Kuthanazhi, J. John, C. S. Solanki, J. M. Vasi, A. Kumar and O. S. Sastry, “Performance degradation in field-aged crystalline silicon PV modules in different Indian climatic conditions,” in *Proceedings of the 40th IEEE Photovoltaic Speacialists Conference*, Denver.

[35] N. Bosco, T. J. Silverman and S. Kurtz, “Climate specific thermomechanical fatigue of flat plate photovoltaic module solder joints,” *Microelectronics Reliability,* vol. 62, pp. 124-129, 2016.

[36] A. Gok, E. Ozkalay, G. Friesen and F. Frontini, “Power loss modes of building-integrated photovoltaic modules: An analytical approach using outdoor I-V curves,” *IEEE Journal of Photovoltaics,* 2021.

[37] D. Jordan, J. Wohlgemuth and S. Kurtz, “Technology and climate trends in PV module degradation,” in *27th EUPVSEC*, 2012.

[38] R. Dubey, S. Chattopadhyay, V. Kuthanazhi, J. John, B. M. Arora, A. Kottantharayil, K. L. Narasimhan, C. S. Solanki, V. Kuber and J. Vasi, “All-India Survey of Photovoltaic Module Degradation: 2013,” National Centre

for Photovoltaic Research and Education Indian Institute of Technology Bombay National Institute of Solar Energy, 2013.

[39] E. Ozkalay, G. Friesen, M. Caccivio, P. Bonomo, A. Fairbrother, C. Ballif and A. Virtuani, “Operating temperatures and diurnal temperature variations of modules installed in open-rack and typical BIPV configurations,” *IEEE Journal of Photovoltaic,* 2022.

[40] E. Özkalay, A. Virtuani, A. Fairbrother, A. Skoczek, G. Friesen and C. Ballif, “Quantifying performance loss rates of photovoltaic modules using ground-based vs satellite-based meteorological data,” in *EUPVSEC*, 2021.

[41] S. [Online]. Available: https://solargis.com/.

[42] P. Ineichen, “A broadband simplified version of the Solis clear sky model,” *Solar Energy,* vol. 82, no. 8, pp. 758-762, 2008.

[43] “GIS data layers of Global Horizontal Irradiation, Air Temperature and Photovoltaic Electricity Potential,” Solargis, 2017.

[44] M. Mattei, G. Notton, C. Crisfari, M. Muselli and P. Poggi, “Calculation of the polycrystalline PV module temperature using a simple method of energy alance,” *Renewable Energy,* pp. 553-567, 2006.

[45] IEA-PVPS Task13, “Photovoltaic Module Energy Yield Measurements: Existing Approaches and Best Practice,” International Energy Agency, 2018.

[46] IEC, “IEC61724:1998 Photovoltaic System Performance Monitoring—Guidelines for Measurement, Data Exchange and Analysis,” International Electrotechnical Comission, Geneva, 1998.

[47] R. Cleveland, W. Cleveland, J. McRae and I. Terpenning, “STL: A Seasonal-Trend Decomposition Procedure Based on Loess,” *Journal of Official Statistics,* 1990.

[48] S. Lindig, I. Kaaya, K. A. Weis, D. Moser and M. Topic, “Review of Statistical and Analytical Degradation Models for Photovoltaic Modules and Systems as Well as Related Improvements,” *IEEE Journal of Photovoltaics,* vol. 8, pp. 1773-1786, 2018.

[49] D. C. Jordan, C. Deline, S. R. Kurtz, G. M. Kimball and M. Anderson, “Robust PV degradation methodology and application,” *IEEE Journal of Photovoltaics,* vol. 8, pp. 523-531, 2018.

[50] J. Ascencio-Vásquez, J. Bevc, K. Reba, K. Brecl, M. Jankovec and M. Topič, “Advanced PV performance modelling based on different levels of irradiance data accuracy,” *Energies,* 2020.

[51] S. Lindig, D. Moser, A. J. Curran, K. Rath, A. Khalilnejad, R. H. French, M. Herz, B. Müller, G. Makrides, G. Georghiou, A. Livera, M. Richter, J. Ascencio-Vásquez, M. van Iseghem, M. Meftah, D. Jordan, C. Deline, W. van Sark, J. S. Stein, M. Theristis, F. Baumgartner and W. Luo, “International collaboration framework for the calculation of performance loss rates: Data quality, benchmarks, and trends (towards a uniform methodology),” *Progress in Photovoltaics: Research and Applications,* vol. 29, no. 6, p. 573– 602, 2021.

[52] G. Friesen, W. Herrmann, G. Belluardo, B. Herteleer, J. Sutterlütti, A. Driesse, K. Emery and M. Schweiger, “Photovoltaic Module Energy Yield Measurements: Existing Approaches and Best Practice,” International Energy Agency, 2018.

[53] S. Kawai, T. Tanahashi, Y. Fukumoto, F. Tamai, A. Masuda and M. Kondo, “Causes of Degradation Identified by the Extended Thermal Cycling Test on Commercially Available Crystalline Silicon Photovoltaic Modules,” *IEEE Journal of Photovoltaics,* vol. 7, no. 6, pp. 1511-1518, 2017.

[54] A. Fairbrother, H. Quest, E. Özkalay, P. Wälchi, G. Friesen and C. Ballif, “Long-term performance and shade detection in building integrated photovoltaic systems,” *Solar RRL,* 2022.

[55] A. Gok, E. Ozkalay, G. Friesen and F. Frontini, “The Influence of Operating Temperature on the Performance of BIPV Modules,” *IEEE Journal of Photovoltaics,* 2020.